On the initial steps in the decomposition of energetic materials from excited electronic states

H.-S. Im and E. R. Bernstein

Citation: The Journal of Chemical Physics **113**, 7911 (2000); doi: 10.1063/1.1315609
View online: http://dx.doi.org/10.1063/1.1315609
View Table of Contents: http://aip.scitation.org/toc/jcp/113/18
Published by the American Institute of Physics

On the initial steps in the decomposition of energetic materials from excited electronic states

H.-S. Im and E. R. Bernstein
Department of Chemistry, Colorado State University, Fort Collins, Colorado 80523-1872

(Received 19 June 2000; accepted 16 August 2000)

Decomposition studies of hexahydro-1,3,5-trinitro-1,3,5-triazine (RDX-$C_3H_6N_6O_6$, see Fig. 1) isolated in the gas phase and cooled in a supersonic expansion are reported for the excited electronic state near 225 nm. The RDX is handled safely and effectively through matrix-assisted laser desorption (MALD) of a thin film of RDX/R6G laser dye (1:1) adsorbed on an aluminum oxide coating on an aluminum drum. The aluminum oxide coating is generated by plasma electrolytic oxidation of aluminum. The combination of MALD and supersonic molecular beam techniques generates intact and cold RDX molecules isolated in the gas phase. Two basic conclusions are reached in this study. (1) Photodissociation of RDX at ≈225 nm generates NO as an initial product. (2) Nascent NO thus generated is vibrationally hot (T_{vib}~1800 K) and rotationally cold (T_{rot} ~20 K). © *2000 American Institute of Physics.* [S0021-9606(00)01142-9]

I. INTRODUCTION

Hexahydro-1,3,5-trinitro-1,3,5-triazine (RDX-$C_3H_6N_6O_6$, see Fig. 1) is an energetic material with broad applications as an explosive and a fuel. An energetic material is any compound with a C:H:N:O ratio close to 1:1:1:1. This classification includes both cyclic and noncyclic species such as HMX ($C_4H_8N_8O_8$), TNT ($C_7H_5N_3O_6$), TNAZ ($C_3H_4N_3O_6$), ADN ($NH_4N(NO_2)_2$), NA (H_2NNO_2), DMNA ($(CH_3)_2NNO_2$), and many others.[1] Past studies of energetic material decomposition reactions have focused mainly on the ground electronic state in the condensed phase with the initiation stimulus being such events as thermal pulses, shocks, sparks, and various laser pulses. Experimental, theoretical, and simulation studies have all been pursued.[2] Elucidation of the detailed fundamental steps in the initiation and propagation phases of energetic material decomposition reactions is central for understanding, controlling, and enhancing the performance of these materials as fuels and explosives. The efficient use of these materials for combustion and explosion also presents a number of environmental issues. Additionally, such an in-depth and molecular understanding of the chemistry of energetic materials should lead to suggestions concerning their performance enhancement and even new candidate molecules for synthesis.

Unimolecular fragmentation and pathways and energy partitioning amongst product species and degrees of freedom depend sensitively on the state of the reactant molecule. Even for similar systems such as nitro-containing aromatics, alkanes, nitramines, saturated heterocyclics, etc., initial products of the dissociation process can very considerably; for example, the first step in dissociation can yield HONO, NO_2, NO, NNO_2, CH_2NNO_2, . . . , depending on reactant energy content, partitioning (electronic, vibrational, rotation), and state. These issues become particularly compelling for the rapid decomposition of highly energetic molecules such as RDX.

The decomposition of energetic materials can be initiated with a shock wave or a spark into a solid sample. In both cases, very large electric fields (≈10^8 V/cm) are generated as crystal planes sheer or as the spark propagates. Such events in solids generate molecules in highly excited electronic states. Clearly, the decomposition of solid energetic materials under shock, spark, laser, or plasma ignition must include contributions from both ground and excited electronic state species. Excitation in the UV can markedly reduce the power requirements for detonation of some secondary explosives. Therefore, elucidation of the initial steps of RDX decomposition from excited electronic states is an important goal to pursue.

A number of experimental and theoretical studies have been conducted to investigate the physicochemical properties of RDX.[3] To date, the majority of decomposition studies of energetic materials are for the ground electronic state. In addition, a variety of prototype, model energetic molecules has been examined to explore the kinetics and reaction mechanisms of the decomposition processes.[4] Different mechanisms have been suggested for the decomposition of RDX, depending on the initiation processes, system phase, and the physical condition of RDX. Nitramine (N–N) bond rupture,[5] the concerted decomposition into CH_2NNO_2,[6] internal ring formation and HONO generation,[5(a)] and other heterogeneous mechanisms[7] have all been proposed.

Most of the RDX decomposition studies in condensed phase have suggested that C–N bond rupture is its primary reaction step to give NO, N_2O, H_2, CO, CH_2O, and CO_2.[8] One study suggests that C–H bond breakage is the rate-determining step for RDX decomposition.[9] An x-ray photoelectron spectroscopy study of shock-induced decomposition of powered RDX shows that N–N bond scission occurs in such samples.[10] When decomposition is studied at higher temperatures producing gas phase molecules, two other mechanisms predominate. The first pathway involves an NO_2 stripping mechanism in which all three NO_2 groups are removed before the triazine fragment decomposes to form

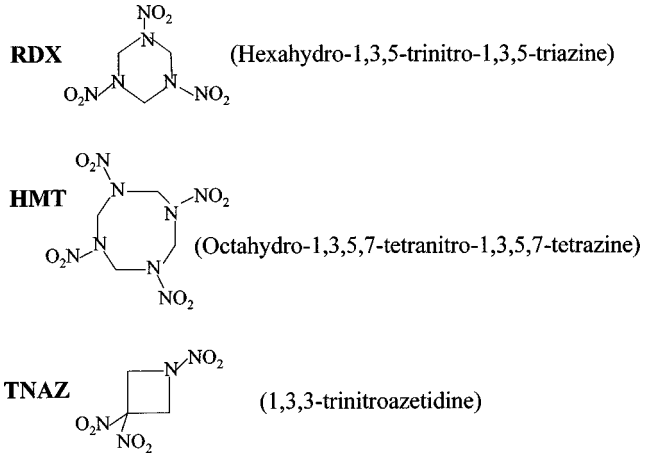

FIG. 1. Molecular structures of RDX and other energetic materials.

HCN and, presumably, H_2.[5(b)] The second pathway, which clearly has been identified as a concerted reaction in molecular beam studies,[6] is a symmetric triple fission to form CH_2NNO_2 fragments that then further decompose to form CH_2O and N_2O. From the study of 248 nm photodecomposition of RDX, another interesting initial step has been proposed through the observation of OH emission.[5(a)] The most likely mechanism for OH production is unimolecular decomposition of RDX via a five-membered ring formation (CHONN). The immediate precursor of OH in this mechanism is probably the primary fragment HONO. Depending on the experimental conditions, eventually all the above possible six pathways can be suggested as an initial step for the decomposition of RDX. Since these studies have been conducted with solid RDX or highly heated RDX (mostly above 200 °C), the behavior of single RDX molecules is difficult to extract. Solid state chemical reactions or thermal decomposition reactions could control and mask the behavior of single RDX molecules.

Through studies of intact, isolated RDX molecules, one can access such fundamental information as unimolecular decomposition pathways, decomposition rates, and energy distributions of the initial species in the reaction/fragmentation processes. This information will serve as a reference point from which to consider and analyze condensed phase behavior and various applications under standard ignition conditions. In order to study the decomposition of an individual RDX molecule from excited electronic states, intact RDX molecules should be generated and entrained in a supersonic molecular beam. Under these conditions, one can remove the effect of intermolecular interactions on decomposition. Matrix-assisted laser desorption ionization (MALDI) has proved to be a viable technique to obtain intact molecular ions of medium size molecules in the gas phase.[11] In addition, intact neutral molecules can be produced with this technique for nonvolatile and fragile large molecules (MALD process). The combination of MALD and supersonic molecular beam techniques enables optical spectroscopy studies for individual molecules that cannot be investigated otherwise.[12]

In the present work, MALD has been successfully combined with molecular beam techniques. The sample preparation method and the proper experimental parameters are established to obtain constant and stable sample introduction for more than 6 h. The desorption laser beam ($\sim 10^6$ W/cm^2) does not disturb the molecular beam dynamics from the nozzle. This setup is applied to the dissociation study of an explosive, RDX. In our studies thus far, we follow the initial NO product of RDX dissociation from excited state potential energy surfaces and characterize its rotational, vibrational, and electronic states. The basic conclusions we reach are that (1) product NO is vibrationally hot ($\sim$1800 K) but is rotationally cold ($\sim$20 K) in the dissociation process at $\approx$44 200 cm^{-1} of RDX excitation energy, and (2) intact and cold RDX can be obtained by the combination of matrix-assisted laser desorption (MALD) and molecular beam techniques. By comparing the NO signals for photofragmented model systems, CH_3NO_2, $C_6H_5NO_2$, $C_6H_4(NO_2)_2$, NO_2, and HONO, the dynamics of RDX in excited electronic states can be investigated to determine that NO is fragmented directly from the photolysis of RDX using UV photons above 38 650 cm^{-1} in energy.

II. EXPERIMENT

In order to obtain a supersonic molecular beam of nonvolatile, thermally unstable solid samples like RDX, a laser desorption (LD) approach is adapted and combined with the supersonic jet technique. The desorbed molecules must be efficiently entrained in the high-pressure throat region of a pulsed supersonic expansion to produce sufficient jet cooling to give well-resolved rovibronic spectra. In our experiment, this is accomplished using a desorption nozzle assembly similar to that described previously by Smalley.[13] In this assembly a LD extension block is attached to a pulsed supersonic nozzle (Jordan Company, PSV).

The desorbed molecules are released and entrained into supersonic expansion within the extension block. The extension block consists of a stepper motor and gears, a shaft for a sample holder, a sample holder, a flow channel, a laser beam inlet hole, and a laser beam alignment hole. At the center of the extension block, a flow channel of 2 mm diam and about 6 cm long is aligned with the nozzle orifice (2 mm diam). This flow channel does not change the supersonic nozzle performance significantly, although the final expansion pressure is reduced by a rough factor of 5–10. The rotational distribution of small molecules is thus not as narrow as would be expected from an unmodified nozzle; the rotational temperature of NO gas increases to $\approx$11 K from $\approx$2 K with the addition of the laser ablation/desorption extension block to the normal supersonic nozzle. For large molecules, this effect is negligible.

The ablation laser beam inlet channel of 1 mm diam is perpendicular to the gas/sample flow channel. The sample holder is made of Al and has a right circular cylindrical shape. The dimensions of the Al drum are 38.79 mm and 27.03 mm for the outer diameter and the inner diameters, respectively, with a 20 mm height. The sample drum is installed in the extension block on a shaft that can be simultaneously rotated and translated through the combination of a

stepper motor and gears. The whole sample holder setup is designed for the sample surface to be tangential to the gas flow channel.

The use of laser desorption as a source of molecules for laser spectroscopy requires the production of a stable supply of sample vapor pulses for extended periods of time. This condition can be achieved by preparing a porous and smooth surface for even deposition of a sample. In our experiments, such a surface is obtained using an aluminum oxide thin film coated on an aluminum drum. The aluminum oxide thin film is generated by plasma electrolytic oxidation.[14] An Al drum as an anode is immersed into the electrolytic solution, and dc voltage of 120–150 V is applied to maintain a current of 1.0–1.5 A. The electrolytic solution is composed of NaF, $Na_2B_4O_7$, $(NH_4)_2HPO_4$, and NaH_2PO_4 with the concentration of 0.6, 0.1, 0.1, and 0.5 M, respectively. Under these conditions, a plasma is formed on the surface of the Al drum and oxidizes it. A γ-Al_2O_3 film about 10 μm thick can be produced on the Al drum surface within 10 min. The coated surface is smooth with a grain size of less than 10 μm.

Equimolar quantities (4×10^{-5} mol) of the sample and a matrix substance are dissolved in an appropriate solvent, mainly acetone in this experiment. The laser dye R6G is chosen as a matrix substance because of its absorption coefficient at 532 nm. A mixture of RDX or 1,4-dinitobenzene and R6G at 1:1 molar concentration is sprayed on the prepared drum. An air atomizing spray nozzle (Spraying System Co.) with siphon pressure of 20 psig is used to deposit the RDX/R6G sample on the drum surface. During the spraying, the drum is heated with a halogen lamp to help solvent dry and rotated with a clock motor for homogeneous coating.

The prepared sample is placed in the extension block and irradiated with a 532 nm laser beam focused with a 1000 mm focal length lens. The desorption spot is approximately 2.75 cm downstream from the nozzle orifice. The laser beam radiant energy right after the lens is set to be about 300 μJ/pulse by putting an orifice of 1–3 mm in front of the lens. The laser intensity is determined by dividing the laser beam radiant energy measured with an Ophir PE10-SH pyroelectric probe by the laser beam pulse width ($\sim$7 ns) and the laser beam area at the sample holder surface. The size of the laser beam spot on the sample holder surface is adjusted to be 1.0 mm diam at the sample holder surface. This yields the laser intensity of about 5×10^6 W/cm^2. As depicted in Fig. 2, NO gas distribution in the supersonic beam with the LD laser on is almost same as that with the LD laser off. The pulse shape and width of 50 μs FWHM is typical of this kind of commercial pulsed valve.

Desorbed, undissociated molecular vapor is entrained in a supersonic molecular beam of 10% Ar/He. By rotating and translating the sample drum, fresh sample can be supplied continuously for each laser shot. With the given size drum, fresh sample can be supplied for more than 6 h continuously. About 3.25 cm downstream from the desorption spot the desorbed molecules entrained in the carrier gas flow into a vacuum chamber and are carried by ensuing molecular beam through a 2 mm skimmer into the ion source of a Willey–McLaren-type time-of-flight mass spectrometer (TOFMS).

Another laser is used to probe the desorbed sample molecules. In this experiment, the probe laser is applied to induce photodissociation of sample molecules and to ionize photodissociated NO via its $A(v'=0,1)\leftarrow X(v''=0-3)$ and $I\leftarrow A$ transitions. The NO^+ is then detected, mass selectively, in the TOFMS. If necessary, the laser beam is focused by a lens of 360 mm focal length. In order to obtain the proper UV photons for this process, a dye laser output is doubled and then mixed with the fundamental output of a Nd:YAG laser. The frequency doubled output (532 nm) of the fundamental (1.064 mm) Nd:YAG laser (Spectra Physics, GCR-3) is used for pumping the dye laser. The four dyes required to cover the NO $A\leftarrow X$ transitions are a mixture of R610 and R590 for (0–0) and (1–1), R640 for (0–1), DCM for (0–2), and LDs 689 for (1–3) and (0–3). Energy of the UV laser output is 0.2–0.5 mJ/pulse depending on the exact wavelength of interest. This implies that the laser intensity becomes $1.3-2.1\times10^8$ W/cm^2 as the laser beam is focused with a lens of 360 mm focal length.

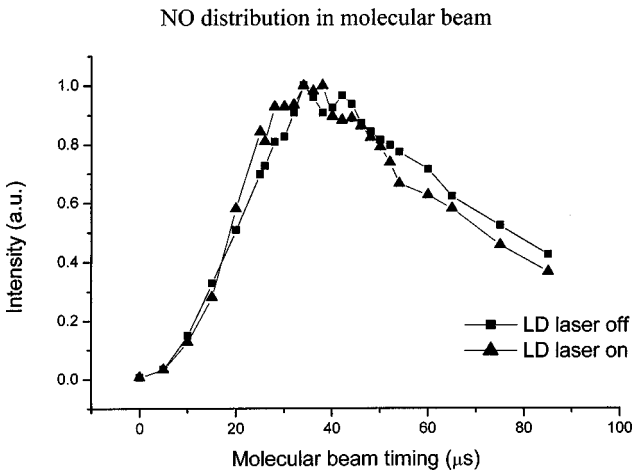

FIG. 2. NO distribution in the molecular beam of our MALD supersonic nozzle with and without LD laser.

Timing of the pulsed valve and the probe laser relative to the desorption laser is controlled through time delay generators (SRS, DG535). The NO^+ ions detected by the microchannel plate (MCP) in TOFMS are recorded on a PC through an ADC card (Analog Devices, RTI-800) and a boxcar averager (SRS, SR250). For velocity distribution measurements, the chamber working pressure and pulsed valve timing are kept constant and unchanged as the timing of the probe laser is swept. The detailed experimental scheme is depicted in Fig. 3.

In order to estimate the vibrational temperature of photofragmented NO from RDX, a Boltzmann distribution calculation is applied using the ratios of each vibronic transition intensity to that of the 0_0^0 transition. To estimate the rotational temperature of NO, the rotation spectrum of the 0_0^0 transition is simulated with the estimated temperature using diatomic molecular rotational level calculation software developed at Sandia National Laboratory.[15]

RDX is received from Lawrence Livermore Laboratory and used without any further treatment. R6G dye is purchased from Eastman Kodak Co. and is used as received. For one experiment, 10 mg of RDX and 25 mg of R6G are

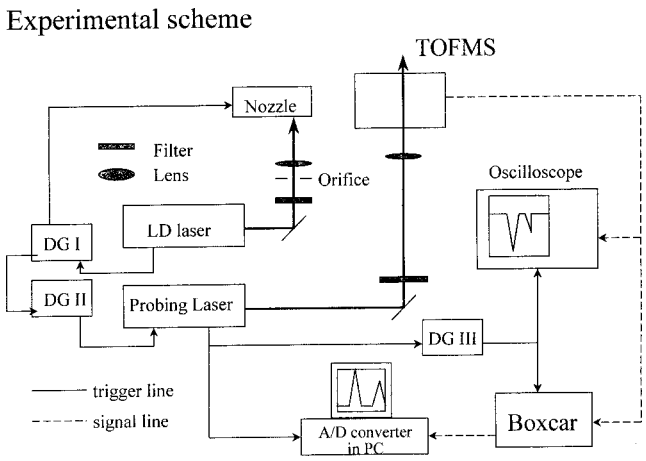

FIG. 3. Schematic drawing of experimental setup for the present work (DG =delay generator).

dissolved in acetone and sprayed. Other samples are examined to determine and prove the source of NO. These samples are NO gas, NO_2 gas, nitromethane (NM), nitrobenzene (NBZ), and 1,4-dinitrobenzene (DNBZ). All are purchased from Aldrich and used without any further treatment. For the NO_2 gas experiment, a significant amount of oxygen gas (10%) is included in the sample vessel in order to suppress the formation of NO as a contaminant. The mixture of NO_2 (0.5%) and O_2 (10%) is prepared in He gas premixed with 10% Ar. This mixture is delivered through PVC tubing to the pulsed valve and then expanded into the vacuum chamber with a total pressure of 100 psig through the above described nozzle with and without the extension block for MALD. In order to generate enough vapor pressure, NBZ is heated to 40 °C. The laser desorption technique is also used for hexamethylenetetramine (HMT), tyramine, and DNBZ to test the process. For all the samples, He gas is premixed with 10% Ar and used as the expansion gas at a total pressure of 100 psig.

III. RESULTS AND DISCUSSION

Spectra of NO excited from $X(v''=0,1,2,3)$ to $A(v'=0)$ are obtained from laser desorbed RDX as presented in Fig. 4. All the spectra show almost the same pattern except for intensity; each spectrum shows one strong peak, which can be assigned as the $(Q_{11}+P_{21})$ band for each vibrational transition,[16] and other lower intensity rotational peaks that are spread within 100 cm^{-1} about the $(Q_{11}+P_{21})$ band. Such a pattern can also be observed for the other transitions, like the (1–1) and (1–3) transitions, for example, as shown in Fig. 5. From the simulation of the NO (0–0) rotational spectrum, the rotational temperature of NO from RDX can be estimated as $T_{rot}=\sim 20$ K (see Fig. 6). NO gas, under the same expansion conditions, is found to have a rotational temperature of ~11 K.

A strongly wavelength-dependent signature is obtained for the NO $A\leftarrow X$ vibronic transitions due to the populations of $v''=0,1,2,3$. In an attempt to obtain $A\leftarrow X$ (0–4) spectrum, no significant signal is observed. The ratio of the intensities of the $(Q_{11}+P_{21})$ band of each vibration are $(v''=0):(v''=1):(v''=2):(v''=3)=1:0.22:0.05:0.02$. These values are quite different from a Boltzmann population distribution of $T=300$ K and below. These observed ratios can be well fitted to a Boltzmann distribution with a temperature of about 1800 K. This fitting is represented in Fig. 7. For NO gas itself, the transitions from $v''=2,3$ cannot be observed. In addition, the molecular beam distribution of NO from the laser desorbed RDX is different from that of NO gas. As displayed in Fig. 8, only a distribution width of 10 μs FWHM can be produced for NO from the laser desorbed RDX. A 50 μs FWHM distribution is detected for NO gas, as is typically for this kind of commercial nozzle. These experimental results clearly indicated that the detected NO molecules are not from NO contamination, but are related to the generation/photolysis of RDX.

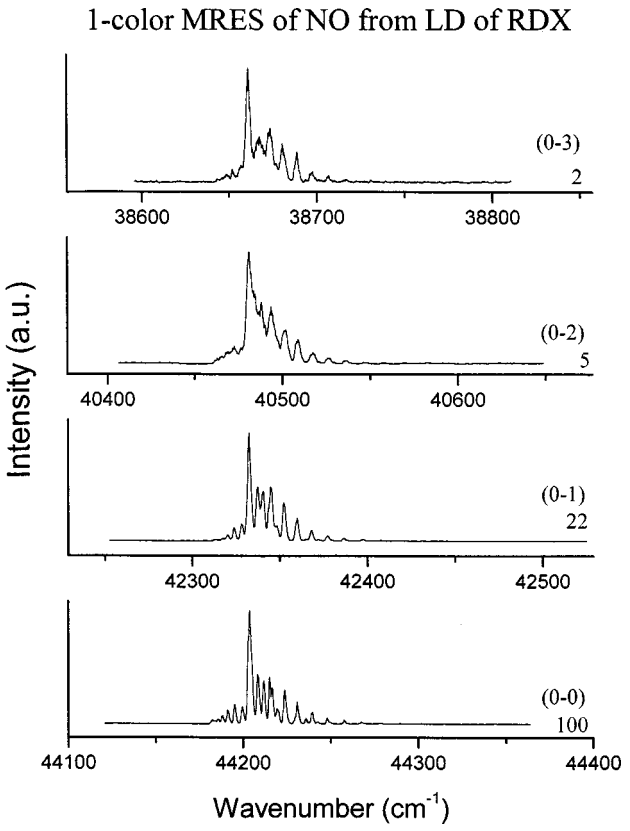

FIG. 4. NO spectra $A\ (v'=0)\leftarrow X\ (v''=0,1,2,3)$. Each transition and its relative intensity to the NO (0–0) transition are indicated in the figure. NO is generated from the photodissociation of RDX.

Since the laser desorption process is employed in the present experiment, however, the above results do not distinguish, in principle, whether the photolysis of RDX occurs at the ionization region of TOFMS or at the LD sampling region within the extension block. If fragmented NO is produced in the latter instance, it would be entrained in the backing gas and expanded to the ionization region. The NO spectrum obtained through this process should be nearly the same as that obtained from NO gas from a supersonic nozzle. If the photolysis of RDX would happen at the ionization region of TOFMS, on the other hand, it would provide different NO molecules from these provided by NO gas molecular supersonic jet expansion. In this case, the spectrum of

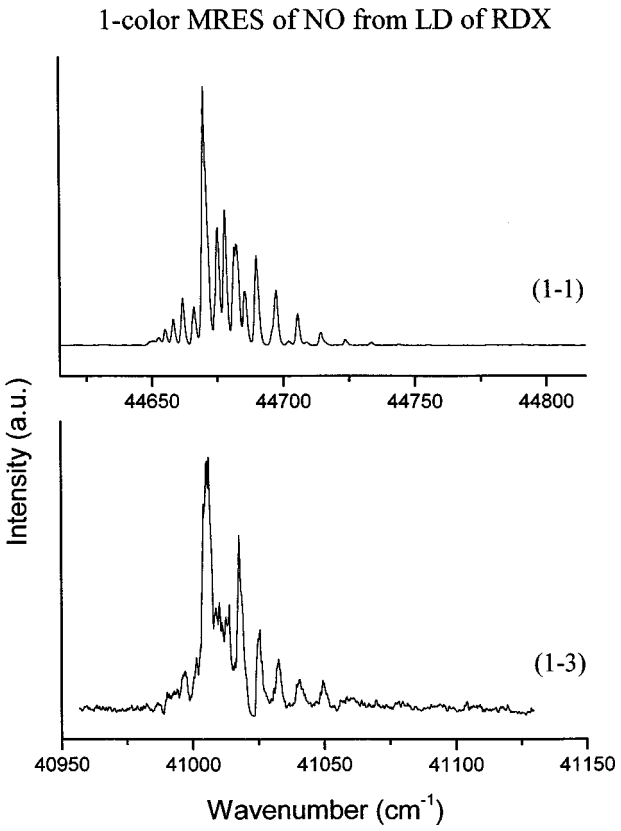

FIG. 5. NO/RDX spectra of the (1–1) and (1–3) transitions. These spectra look very similar to the other transitions obtained from nascent NO derived from RDX photodissociation (see Fig. 4).

fragmented NO should be substantially different from that of NO gas from a supersonic nozzle. In Fig. 9, the spectra at the (0–1) transition are clearly not the same; the rotational temperature of NO from the desorption of RDX is much lower than that found for NO gas from a supersonic expansion nozzle. This result implies that the fragmented NO is

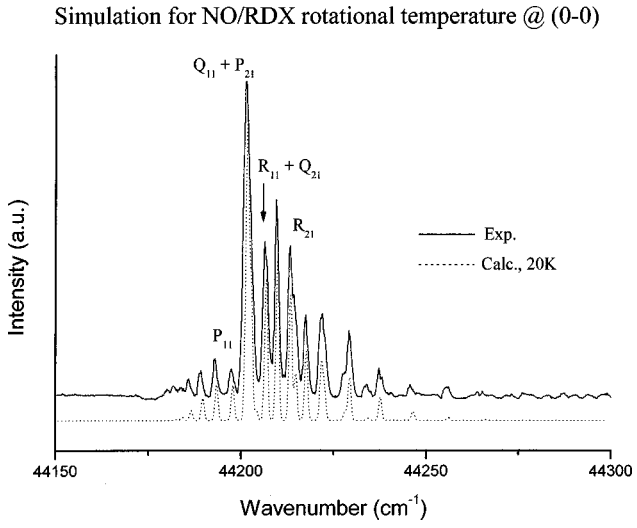

FIG. 6. Simulation of the NO rotational spectrum at the (0–0) transition obtained by RDX photolysis. The dotted line is the simulated spectrum fit to the experimental spectrum (solid line). The rotational temperature is determined to be 20 K.

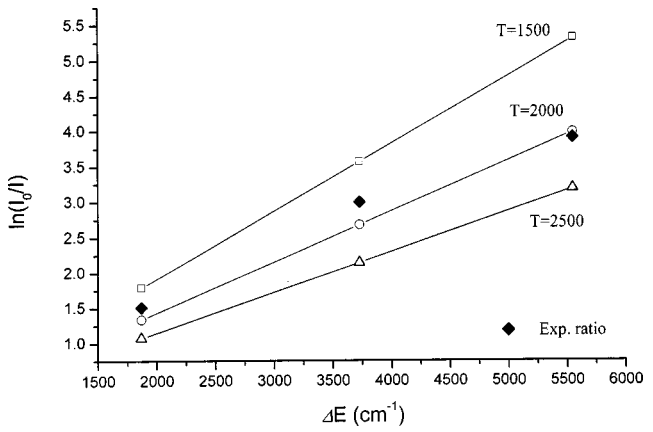

FIG. 7. Boltzmann distribution calculation for determining the vibrational temperature of fragmented NO from photolysis of RDX. Ratios of the $(Q_{11}+P_{21})$ band intensity of each vibrational transition to that of (0–0) are used to determine $T_{\mathrm{vib}}\sim 1800$ K.

generated from the photolysis of RDX at the ionization region. The logic behind this conclusion is as follows: (1) NO from RDX MALD has $T_{\mathrm{vib}}\sim 1800$ K, so the vibrational cooling of NO is not very good if the NO comes from the nozzle; (2) the rotational cooling of NO from RDX MALD is very good as T_{rot} (0–1)$\sim$20 K; (3) but nozzle cooling of gaseous NO gives T_{rot} (0–1)$\sim$100 K and $T_{\mathrm{vib}}\sim 200$ K; and (4) therefore, assuming NO from RDX MALD comes from the nozzle and not the TOFMS ion source presents a logical inconsistency with hot vibrational levels and cold rotational levels from the same nozzle. Apparently, rotational and vibrational cooling of gas phase NO expanded from our nozzle are comparable for the higher vibrational level $X\ (v''=1)$, so the only way that NO from RDX MALD could have $T_{\mathrm{vib}}\sim 100$ T_{rot} is if this temperature disparity exists in the dissociation process. The following velocity slip experiment confirms the present interpretation and proves that NO is generated at the TOFMS ionization region.

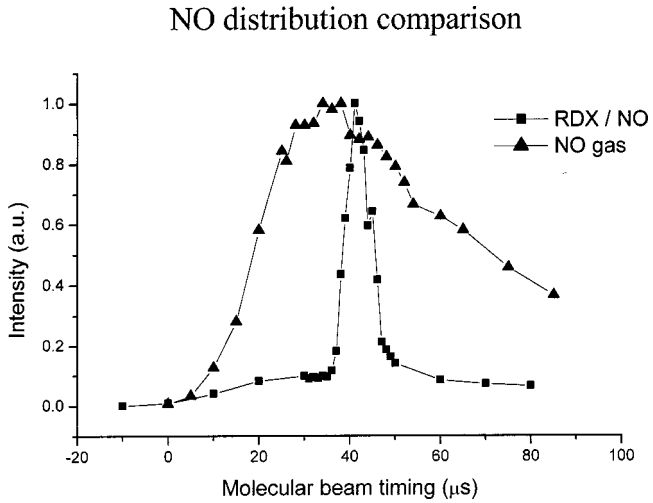

FIG. 8. A comparison between the detected distributions of NO TOFMS intensity from two different sources: (1) Gas phase NO expanded through a supersonic nozzle (triangles); and (2) gas phase NO derived from MALD-generated RDX fragmented at the TOFMS ion source region (squares).

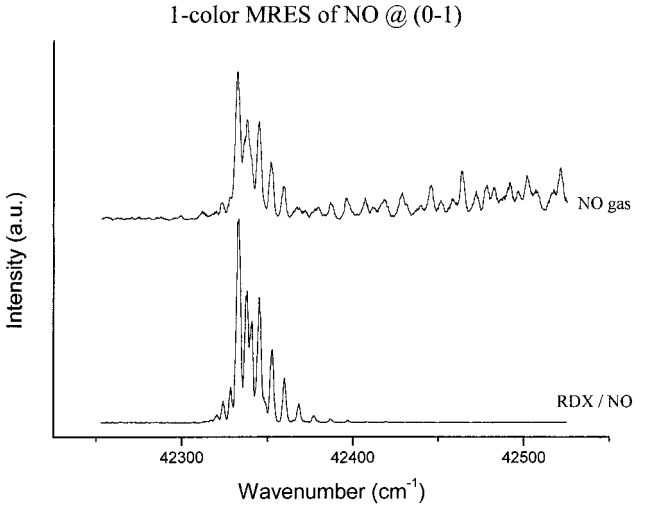

FIG. 9. NO spectra of the (0–1) transition from NO fragmented from RDX photolysis (bottom) and from NO gas itself (top). NO spectrum from RDX fragmented NO displays a much colder rotational temperature than NO gas itself.

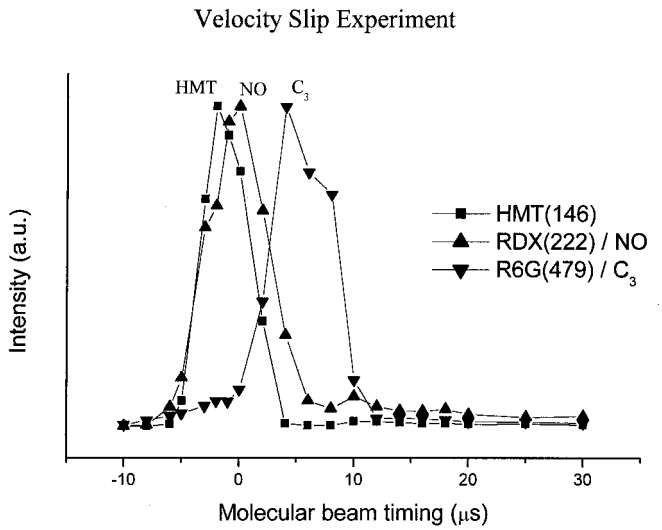

FIG. 10. Velocity distribution differences among laser desorbed HMT, RDX, and R6G. Equimolar quantities of HMT and RDX samples are coated together with the matrix molecule, R6G. Signals from the parent molecule for HMT, NO for RDX, and C_3 for R6G have been used to determine the velocity distribution data.

In a molecular beam, the velocity distribution of a sample molecule is known to be dependent upon its molecular mass; light molecules travel faster than heavy ones. This timing shift of the velocity distribution (the velocity slip) in the molecular beam has been used to match photofragmented species to their parent molecules.[17] The velocity distribution of the photofragmented NO from laser desorbed RDX shows a different arrival time compared to that of NO gas itself or other vapor samples examined. The velocity distributions of gas phase molecules are almost matched to the gas pulse shape of the commercial pulsed valve, the FWHM of the distribution is about 50 μs; however, that of the photofragmented NO is about 10 μs as seen in Fig. 8. This value is exactly the same as the velocity distribution of laser desorbed hexamethylenetetramine (HMT). Also, the photofragmented C_3 from R6G, which is the matrix compound used, shows exactly the same velocity distribution; the FWHM is about 10 μs. Even though the pattern of each velocity distribution looks the same, a velocity slip is observed. The maximum intensity position of HMT (mass 146) is about 2 μs earlier than that of RDX (mass 222), while that of R6G (mass 479) is about 4 μs later, as depicted in Fig. 10. One should note that this measurement has been conducted with NO for RDX, C_3 for R6G, and the parent molecule for HMT at the ionization region of the TOFMS. These observations make clear that the photofragmented NO species has come from a molecule that is heavier than HMT and that is lighter than the parent molecule for C_3, R6G. In this experiment, such a molecule must be RDX.

Therefore, these results [that is, the velocity distribution, the spectrum of NO $A \leftarrow X$ at (0–1), and the velocity slip data] lead to the conclusion that the photofragmented NO species from RDX is generated at the ionization region of the TOFMS. This fact indicates that, using a MALD technique, intact gas phase RDX can be generated from the solid and entrained in the supersonic beam. This allows the initial fundamental steps in the decomposition of isolated RDX from its excited electronic states to be investigated.

Even though the above results determine that the source of NO is the photolysis of isolated, gas phase RDX, they do not reveal the initial reaction pathway that produces NO. When the photolysis of RDX occurs, it could produce several possible fragmented products as the initial step in the dissociation to generate NO. Since these processes could happen within several hundred femtoseconds, one cannot distinguish each step, if a multistep process occurs, using a ns laser. From previous studies on the dissociation of RDX by thermal or laser photolysis,[5–10] one can choose several species as possible candidates for a primary product; these include NO_2, HONO, or CH_2NNO_2. In order to investigate the initial step of the photodissociation of RDX, several model systems, such as NO_2, NO, NBZ, and DNBZ, are examined. NBZ and DNBZ are chosen for a potential intermediate source of HONO; previous studies[18] show that HONO can be an intermediate for NO production through five-membered ring formation in these molecules. The NO spectra obtained from the photolysis of these model systems can be compared to that from the photolysis of RDX. This comparison will serve as a guide to determine potential, appropriate intermediates, if they exist, because the final NO state will be determined from the species found to generate NO directly. Different pathways will result in different intermediates for RDX*$\rightarrow\rightarrow\rightarrow$NO reaction, if they exist.

In Fig. 11, the NO spectrum of the (0–1) transition from the photolysis of RDX is compared with those from NO_2, NM, NBZ, and DNBZ photodissociation. The MALD technique is applied for DNBZ. Each NO spectrum is obviously different from that of fragmented NO from RDX. Photolysis of all the model systems produces highly excited rotational spectra of fragmented NO. NM is well known to have the intermediate NO_2 (that is, $CH_3NO_2+h\nu\rightarrow NO_2$, $NO_2+h\nu\rightarrow NO+O$); at the first step of the dissociation, NO_2 production is a major pathway for the CH_3NO_2 molecule.[19] This

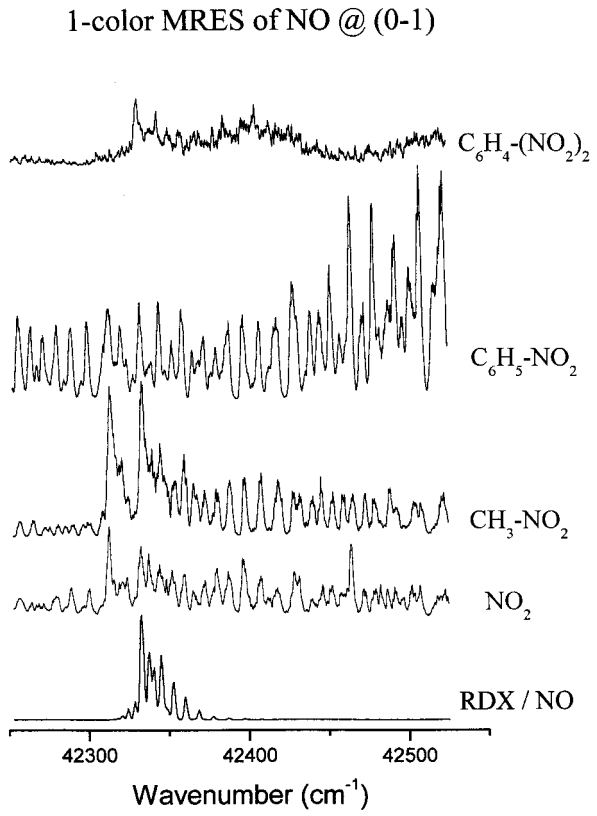

FIG. 11. NO spectra of the (0–1) transition from various model samples (from the bottom to top): RDX photolysis, NO_2, CH_3NO_2, $C_6H_5NO_2$, and 1,4-$(NO_2)_2C_6H_4$). Each molecule shows its own pattern of NO rotational transitions. This means that each molecule has its own unique pathway for NO generation.

fact is supported by our results; the fragmented NO spectrum of NM resembles very closely that of NO_2 (see Fig. 11). The NO spectra from NBZ and DNBZ are different from those generated by RDX and NO_2 and, in fact, from one another. These differences indicate that the dissociation pathways of these molecules are much more complicated than the others, and do not just produce NO_2 or NO during the dissociation. At this point, however, one cannot be certain that HONO is the intermediate for NBZ and/or DNBZ dissociation. Additionally, for NO_2 and NM photodissociation, the transition from $v''=2$ can be observed very easily, while no transition from $v''=3$ can be observed. $A \leftarrow X$ transitions up to $v''=3$ are reported for NBZ, but the NO spectrum from NBZ does not resemble any of the other spectra. The transition from $v''=3$ is observed for RDX (see Figs. 4 and 5). These model systems should have their own unique pathways through which excited state dissociation occurs. One can confirm from these results that NO_2 or CH_2-N-NO_2 should not be an intermediate species in the photodissociation of excited electronic state RDX. Vibrationally hot, but rotationally cold NO molecules may well be produced directly from the dissociation of RDX using UV photons (about 38 650 cm^{-1}, 258.7 nm), but one cannot completely dismiss the possibility of the HONO molecule as an intermediary, because the NBZ, DNBZ$+h\nu \rightarrow$HONO studies were performed at high temperature and pressure. The NO thus generated, however, from HONO at the $v''=1$ state is rotationally very hot.[18(a)] We will begin studies of HONO photodissociation in the near future to determine photofragmented NO T_{vib} and T_{rot} from cold HONO. In order to determine the exact pathway of RDX dissociation in excited electronic states, time-resolved measurements using ultrafast, fs probing will be conducted in the near future. This method will allow both fragment species and RDX itself to be accessed by mass spectroscopy.

IV. CONCLUSIONS

In order to study optical spectroscopy for nonvolatile and fragile large molecules, MALD has been successfully combined with a molecular beam supersonic expansion technique. Sample preparation methods and proper experimental parameters are established to obtain constant sample introduction for more than 6 h. LD laser beam intensity ($\sim 10^6$ W/cm^2) does not disturb the molecular beam dynamics in the nozzle. In the present study, this setup is applied to investigate photodissociation of an explosive, RDX. The present experimental results lead us to conclude the following:

(1) Intact and cold RDX can be obtained by the combination of matrix-assisted laser desorption (MALD) and molecular beam techniques;
(2) Photolysis of RDX produces vibrationally hotter ($T_{vib} = \sim 1800$ K), but rotationally colder ($T_{rot} = \sim 20$ K) photofragmented NO compared to that from NO gas itself or other NO_2-compared molecules;
(3) By comparing the NO signal among the model systems, the dynamics of RDX in excited states can be investigated to determine that NO is probably fragmented directly from RDX using UV photons of higher than 258 nm (above 38 650 cm^{-1}) and that NO_2 and CH_2NNO_2 are not intermediates in this process.

RDX is a true energetic material and apparently has a distinct dissociation pathway that is different from those of the model systems compared to it in this investigation.

ACKNOWLEDGMENTS

This research is supported by the USARO. We wish to thank Dr. R. Simpson for supplying the RDX for this work. We thank Dr. G. J. Stueber for making available to us the technique of plasma electrolytic oxidation and pointing out to us Ref. 14.

[1] (a) T. B. Brill, T. P. Russell, W. C. Tao, and R. B. Wardle, *Decomposition, Combustion, and Detonation Chemistry of Energetic Materials*, MRS Symposium Proceedings (Material Research Society, New York, 1996), Vol. 418; (b) G. F. Adams and R. W. Shaw, Jr., Annu. Rev. Phys. Chem. **43**, 311 (1992); (c) G. A. Olah and D. R. Squire, *Chemistry of Energetic Materials* (Academic, San Diego, 1991); (d) *Chemistry and Physics of Energetic Materials*, edited by S. N. Bulusu (Kluwer Academic, The Nederlands, 1990).
[2] V. Swayambunathan, S. Singh, and R. C. Sausa, Appl. Opt. **38**, 6447 (1999), and references therein.
[3] (a) K. J. Smit, J. Energ. Mater. **9**, 81 (1991); (b) S. N. E. Bulusu, *Chemistry and Physics of Energetic Materials*, NATO ASI Series C (Kluwer, Dordrecht, 1990), Vol. 309; (c) Y. Oyumi and T. B. Brill, Combust. Flame **62**, 225 (1985); (d) F. I. Dubovitskii and B. L. Korsunskii, Russ. Chem. Rev. **50**, 958 (1981); (e) J. D. Cosgrove and A. J. Owen, Combust. Flame **22**, 13 (1974); (f) F. C. Fauch and A. J. Fanelli, J. Phys. Chem. **73**, 1604

(1969); (g) A. J. B. Robertson, Trans. Faraday Soc. **45**, 85 (1949).
[4] Y.-X. Zhang and S. H. Bauer, Int. J. Chem. Kinet. **31**, 655 (1999), and references therein.
[5] (a) C. Capellos, P. Papagiannakopoulos, and Y.-L. Liang, Chem. Phys. Lett. **164**, 533 (1989); (b) C. Capellos, S. Lee, S. Bulusu, and L. Gams, *Advances in Chemical Reaction Dynamics* (Reidel, Dordrecht, 1986), pp. 398–404; (c) H. Zuckermann, G. D. Greenblatt, and Y. Hass, J. Phys. Chem. **91**, 5159 (1987); (d) M. D. Pace and W. B. Moniz, J. Magn. Reson. **47**, 510 (1982).
[6] (a) X. Zhao, E. J. Hinsta, and Y. T. Lee, J. Chem. Phys. **88**, 801 (1988); (b) T. Sewell and D. L. Thompson, J. Phys. Chem. **95**, 6223 (1991).
[7] (a) R. Behrens, Jr. and S. Bulusu, J. Phys. Chem. **96**, 8877 (1992); (b) **96**, 8891 (1992); (c) T. B. Brill, P. E. Gongwer, and G. K. Williams, *ibid*. **98**, 12242 (1994).
[8] (a) J. Alix and S. Collins, Can. J. Chem. **69**, 1535 (1991); (b) M. Farber and R. Srivastava, Chem. Phys. Lett. **64**, 30 (1979).
[9] S. Bulusu, D. Weinstein, J. Autura, and R. Veliky, J. Phys. Chem. **90**, 4121 (1986).
[10] F. J. Owens and J. Sharmar, J. Appl. Phys. **51**, 1494 (1979).
[11] (a) A. Meffert and J. Grotemeyer, Ber. Bunsenges. Phys. Chem. **102**, 459 (1998); (b) K. W. D. Ledingham and R. P. Singhal, Int. J. Mass Spectrom. Ion Processes **163**, 149 (1997), and references therein; (c) R. J. Conzemius and J. M. Cepellen, Int. J. Mass Spectrom. Ion Phys. **34**, 197 (1980), and references therein.
[12] (a) F. L. Plows and A. C. Jones, J. Mol. Spectrosc. **194**, 163 (1999); (b) A. C. Jones, M. J. Dale, G. A. Keenan, and P. R. R. Langridge-Smith, Chem. Phys. Lett. **219**, 174 (1994); (c) M. J. Dale, A. C. Jones, P. R. R. Langridge-Smith, K. F. Costello, and P. Cummins, Anal. Chem. **65**, 174 (1993); (d) G. Meijer, M. S. de Vries, H. E. Hunziker, and H. R. Wendt, J. Chem. Phys. **92**, 7625 (1990); (e) J. Phys. Chem. **94**, 4394 (1990); (f) J. R. Cable, M. J. Turbergen, and D. H. Levy, J. Am. Chem. Soc. **111**, 9032 (1989); (g) **110**, 7349 (1988); (h) L. Li and D. M. Lubman, Appl. Spectrosc. **42**, 418 (1988).
[13] (a) R. E. Smalley, Laser Chem. **2**, 167 (1983); (b) M. Foltin, G. J. Stueber, and E. R. Bernstein, J. Chem. Phys. **111**, 9577 (1999).
[14] (a) G. P. Wirtz, S. Brown, and W. M. Kriven, Mater. Manuf. Processes **6**, 87 (1991); (b) P. Kurze, W. Krysmann, J. Schreckenbach, Th. Schwarz, and K. Rabending, Cryst. Res. Technol. **22**, 53 (1987); (c) W. Krysmann, P. Kurze, K.-H. Dittrich, and H. G. Schneider, *ibid*. **19**, 973 (1984); (d) K.-H. Dittrich, W. Krysmann, P. Kurze, and H. G. Schneider, *ibid*. **19**, 93 (1984).
[15] W. G. Breiland, Sandia National Laboratory, Albuquerque, NM, 1992.
[16] (a) M. Hippler and J. Pfab, Chem. Phys. Lett. **243**, 500 (1995); (b) G. Herzberg, *Spectra of Diatomic Molecules* (Van Nostrand, New York, 1950), p. 257.
[17] (a) Q. Y. Shang, P. O. Moreno, S. Li, and E. R. Bernstein, J. Chem. Phys. **98**, 1876 (1993); (b) S. Li and E. R. Bernstein, *ibid*. **97**, 792 (1992).
[18] (a) C. I. Ning and J. Pfab, J. Phys. Chem. A **101**, 6008 (1997); (b) S. W. Novicki and R. Vasudev, J. Chem. Phys. **95**, 7269 (1991); (c) Chem. Phys. Lett. **176**, 118 (1991); (d) J. H. Shan, S. J. Wategaonkar, and R. Vasudev, Chem. Phys. Lett. **160**, 614 (1989); (e) S. J. Wategaonkar, J. H. Shan, and R. Vasudev, Chem. Phys. **139**, 283 (1989); (f) R. N. Dixon and H. Rieley, *ibid*. **137**, 307 (1989); (g) J. Chem. Phys. **91**, 2308 (1989).
[19] (a) Y.-X. Zhang and S. H. Bauer, J. Phys. Chem. B **101**, 8717 (1997); (b) D. S. Y. Hsu and M. D. Lin, J. Energ. Mater. **3**, 95 (1985); (c) A. Perche, J. C. Tricot, and M. J. Lucquin, J. Chem. Res. **304**, 3219 (1979); (d) K. Galnzer and J. Troe, Helv. Chim. Acta. **55**, 2884 (1972).